

A Fine Delay Measurement Using Forward and Backward Phase Shift for Online Failure Prediction and Analysis

Kentaroh Katoh^{1,a,*}, Toru Nakura^{1,b}, Xiaoqing Wen^{2,c} and Haruo Kobayashi^{3,d}

¹Department of Electronics Engineering and Computer Science, Faculty of Engineering, Fukuoka University, 8-19-1 Nanakuma Jonan-ku, Fukuoka 814-0180, Japan

²Graduate School of Computer Science and Systems Engineering, Kyushu Institute of Technology, 680-4 Kawazu, Iizuka Fukuoka 820-8502, Japan

³Emeritus Professor, Gunma University, 1-5- 1 Tenjin-cho, Kiryu Gunma 376-8515, Japan

* Corresponding author

^a<kentarohkatoh@fukuoka-u.ac.jp>, ^b<nakura@fukuoka-u.ac.jp>, ^c<wen@cse.kyutech.ac.jp>, ^d<koba@gunma-u.ac.jp>

Keywords: on-chip online delay measurement, fine resolution, MUX chain, calibration, phase-variable PLL

Abstract. This paper presents a fine delay measurement using forward and backward phase shift for online failure prediction and analysis. The proposed method uses the secondary shadow clock with the multiplexer (MUX) chain for fine phase shift cascaded with the conventional coarse phase-variable PLL. In the proposed method, first, we perform the coarse slack measurement of target paths based on consecutive path delay test with the forward coarse phase shift with the phase-variable phase locked loop (PLL) clock. Second, we perform the fine slack measurement based on consecutive path delay test with the backward fine phase shift with the MUX chain. The proposed fine and low-cost on-chip delay measurement can be used not only for online prediction of timing failures due to process, voltage, and temperature (PVT) variations and aging, but also for the precise online analysis of failure mechanisms. The experimental results with Artix-7 FPGA of Advanced Micro Devices (AMD) show that the measurement resolution is 10.1 ps. It is 9.7 % of the resolution of the conventional methods. The absolute values of differential non-linearity (DNL) and integral non-linearity (INL) are less than 0.005 least significant bit (LSB).

1. Introduction

Aggressively scaled CMOS process technologies have led to extremely fast and low power processors and system-on-a-chips (SoCs) for high performance handheld devices and AI accelerators. On the other hand, because timing failures caused by PVT variations and aging become serious, it is difficult to guarantee the function of a modern VLSI in field just only with offline testing before shipment [1]. Significant research efforts have been focused on the testing for the online timing failures [2, 3]. Most of them are focused on online failure prediction and analysis [4, 5].

Path delay measurement is useful for both prediction and analysis [6]. In on-chip online path delay measurement, the delay values of a set of critical paths vulnerable to timing failures are measured periodically. The time series of the measured delay data is used for timing failure prediction and analysis of failure mechanisms, such as the analysis of relations among delay degradation, workloads to the paths, and PVT variations. Various methods for delay measurement have been proposed [7]. Online path delay measurement with a phase-shift PLL is one of them [8, 9]. However, the resolution of delay measurement of this approach depends on the specification of the used PLL.

This paper presents a fine delay measurement using forward and backward phase shift for online failure prediction and analysis. The proposed method uses the secondary shadow clock with the MUX chain for fine phase shift cascaded with the conventional coarse phase-variable PLL. In the proposed

method, first, we perform the coarse slack measurement of target paths based on consecutive path delay test with the forward coarse phase shift with the phase-variable PLL clock. Second, we perform the fine slack measurement based on consecutive path delay test with the backward fine phase shift with the MUX chain. The proposed fine and low-cost on-chip delay measurement can be used not only for online prediction of timing failures due to PVT variation and aging, but also for the precise online analysis of failure mechanisms.

The rest of this paper is organized as follows. Section 2 explains the proposed method. Section 3 shows the experimental results. Finally, section 4 concludes the paper.

2. Fine Online Delay Measurement Using a MUX Chain

This section presents the detail of the proposed method. 2.1 describes the proposed measurement architecture and the basics of slack measurement. 2.2 shows the MUX chain used for the backward fine phase shift of the proposed slack measurement. Finally, 2.3 describes the scheme of the proposed slack measurement.

2.1 Architecture and Measurement

Figure 1 shows the block diagram of the proposed measurement architecture. The upper part is the circuit under measurement. This circuit consists of 4 Flip-Flops FF₀-FF₃ and a logic block. The input and the output of FF_{*i*} are D_{*i*} and Q_{*i*}, respectively. The inputs EN and CLK are the enable input and the clock input, respectively. When EN = 1, the Flip-Flops work in synchronization with CLK. When EN = 0, they keep the output values. Assuming an implementation with an AMD FPGA, all the Flip-Flops have the enable input EN [10]. However, even when they do not have an enable input, the proposed method can be still implemented.

The signals inside the circuit propagate from left to right. Accordingly, the outputs of FF₀ or FF₁ are the start points of the paths of the circuit. The inputs of the FF₂ or FF₃ are their end points. The bold line connected the output of FF₀ with the input of FF₃ is the critical path of the circuit.

The bottom part is the circuit for the implementation of the proposed measurement. It is composed of a controller, a system clock generator, a PLL clock generator, a MUX chain, and a shadow Flip-Flop SDFP, which is an extra register for the proposed delay measurement. The clock input is connected to the shadow clock SCLK whose phase can be shifted forward and backward for the measurement. The Flip-Flop is named shadow one because it is not used for normal operation. The input of SDFP D_s is connected to the end of the critical path. The proposed method measures the path whose start point is Q₀ and the end point is D_s, which includes the critical path except the segment from the fanout point to D₃. We call the path ‘path under measurement’. The phase of the system clock CLK is fixed to 0. The phase of the PLL clock CLK_{PLL} can be shifted with coarse resolution. The MUX chain is cascaded with the PLL clock generator. The output of the PLL clock generator CLK_{PLL} is connected with the input of the MUX chain IN. The output of the MUX chain OUT is the shadow clock SCLK. The delay of the MUX chain from IN to OUT can be adjusted with fine resolution. Consequently, the phase of the shadow clock can be adjusted in both coarse and fine manners. The delay from IN to OUT of the MUX chain can be measured with calibration.

All the measurement sequences are controlled with the controller. The outputs of the controller synchronize with either CLK or CLK_{PLL}. It has the inputs TEST and TRG. When TEST = 1, the system is in measurement mode; otherwise it is in normal operation mode. The input TRG is the trigger input of path delay test. Path delay test is executed in a synchronized manner with the positive transition of TRG. The output EN of the controller controls the operation of FF₀-FF₃. The output SEN of the controller controls the operation of SDFP. The controller controls the phase of SCLK although it is omitted due to space limitation.

The proposed method measures the delay of a path with repeating Launch-on-Capture (LOC) path delay test of the path under measurement consecutively shifting the phase of SCLK. In LOC path delay test, a transition is launched at the start point of the path which is connected to an output of a Flip-Flop by applying a clock pulse in normal operation mode. The transition arrives at the input of the common shadow Flip-Flop. The path is sensitized based on single-path sensitizable criterion [11]. The shadow Flip-Flop captures the input value in synchronization with SCLK. Figure 2 shows the timing chart of a path delay test for the path under measurement. When TEST = 1, EN becomes 1 for two-clock period in synchronization with the positive transition of TRG. During EN = 1, FF₀-FF₃ work in a synchronized manner with CLK. In the 1st clock inside the 1st period that EN = 1, a positive transition is launched in Q₀. The transition arrives at the end point of the path under measurement through the logic circuit. The input SEN becomes 1 for a clock period and the shadow Flip-Flop SDFF captures the value of the end point of the path under measurement. The timing SCLK captures the value of the end point of the path under measurement is decided with the length of the path and the range of the measurement considered. When TEST = 0, EN and SEN are fixed to 1 and 0, respectively.

The proposed online delay measurement is the foreground one that stops the normal operation temporally before delay measurement. Because it is used for timing failure prediction or analysis of delay degradation, it is enough to get the difference of delay of the path under measurement. In this paper, we do not intend to measure the absolute delay of the path, but try to measure the slack against the timing that SDFF captures the value of the end point of the target path. Figure 3 shows an example of measurement sequences. In this example, the clock period of both CLK and SCLK is T (s). The time t_i (s) of the horizontal axis is defined as $t_i = i \times t_{step}$, where $t_{step} = T/6$. We assume that the path under measurement is fault-free.

The proposed method measures the timing slack with repeating path delay test of the path under measurement by shifting the data capture timing of SDFF with coarse resolution and fine resolution. Let t_s (s) be the initial capture timing of SDFF. When path delay test is executed, a transition is launched in Q₀ in t_3 . The transition arrives at D_s just before t_8 in this example. The shadow Flip-Flop SDFF captures the value of D_s at t_s just before t_{12} .

Now we start the slack measurement. Here the slack is defined as t_s minus the arrival time of transition from the start point of the path under measurement.

First, path delay test is performed with the initial capture timing of SDFF t_s . Let the captured value be the expected value E . Because the arrival time of the transition is before t_s , $E = 1$ in this example.

Second, we repeat path delay test with shifting phase of clock forward by every $2\pi\Delta T/T$ coarsely until the captured value becomes \bar{E} , where ΔT (s) is the coarse shift time step.

- When the clock phase is shifted by $2\pi\Delta T/T$, the capture timing is $t_s - \Delta T$. Because the transition arrives at D_s before $t_s - \Delta T$, the test response is E .
- When the clock phase is shifted by $4\pi\Delta T/T$, the capture timing is $t_s - 2\Delta T$. In this case, the test response is also E .
- However, when the clock phase is shifted by $6\pi\Delta T/T$, the capture timing is $t_s - 3\Delta T$. Because the arrival time of the transition is after $t_s - 3\Delta T$, the test response is \bar{E} in this case. Now we know that the slack is less than $3\Delta T$.

Third, we repeat path delay test with shifting phase of clock backward by every $2\pi\Delta t/T$ until the captured value becomes E , where Δt (s) is the fine shift time step.

- When the clock phase is shifted $-2\pi\Delta t/T$, the capture timing is $t_s - 3\Delta T + \Delta t$. Because the arrival time of the transition is after $t_s - 3\Delta T + \Delta t$, the test response is \bar{E} .
- Next, when the clock phase is shifted by $-4\pi\Delta t/T$, the capture timing is $t_s - 3\Delta T + 2\Delta t$. Because the arrival time of the transition is before $t_s - 3\Delta T + 2\Delta t$, the test response is E .

Finally, we found that the slack is $3\Delta T - 2\Delta t$. In general, when the number of the forward coarse phase shift is n and that of the backward fine phase shift is m , the slack is $n\Delta T - m\Delta t$.

We let the number of the coarse phase shift $n + 1$ deliberately. As a result, the number of the backward phase shift is m' . Then the slack is calculated as $(n + 1)\Delta T - m'\Delta t$. Figure 4 shows the relation among m , m' , Δt , and ΔT . According to this figure, we obtain the equation $(n + 1)\Delta T - n\Delta T = (m' - m)\Delta t$. It consequently gives

$$\Delta t = \frac{\Delta T}{m' - m} \tag{1}$$

Usually, the paths under measurements are single-path sensitizable. Multiple robust sensitizable paths with common end point can be sensitized simultaneously when we want to measure the worst slack [8,11]. The measurement of what and how many paths depends on the kind of circuit and the aim of the measurement in general. For failure prediction, the set of paths are usually chosen by designers.

These paths have higher workload and vulnerable to aging. Because there exist multiple end points to be observed in general, extra Flip-Flops or multiplexers to observe the end points are required. It results in extra area overhead. Therefore, designers should consider the path selection and the extra area for the measurement. As shown in the timing chart of Fig. 2, the shadow flip flops capture the test response in the period when $SEN = 1$. The optimal timing to rise up SEN depends on delay of the redundant wire and the MUX chain. The timing is adjusted with the controller of Fig. 1. The measured slack may contain the effect of aging of the redundant wire. It causes false positive. We can avoid it with measurement of multiple independent paths with common aged redundant wire.

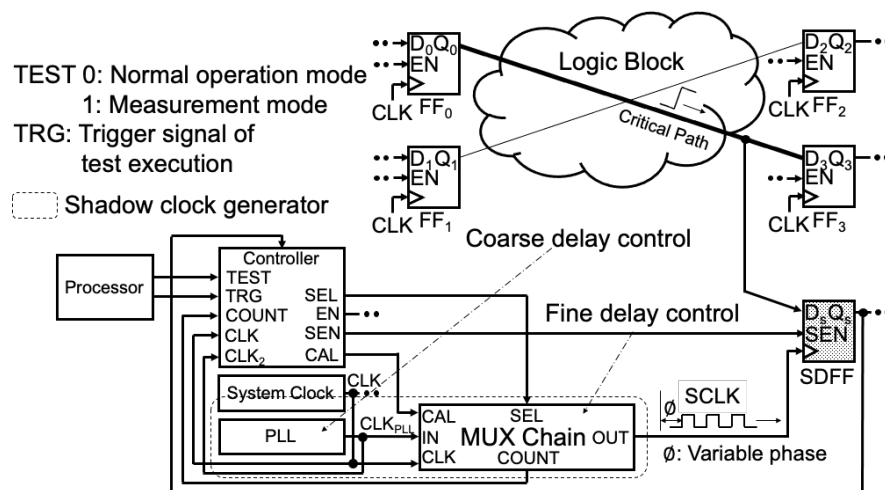


Fig. 1. Architecture of proposed online delay measurement with fine resolution.

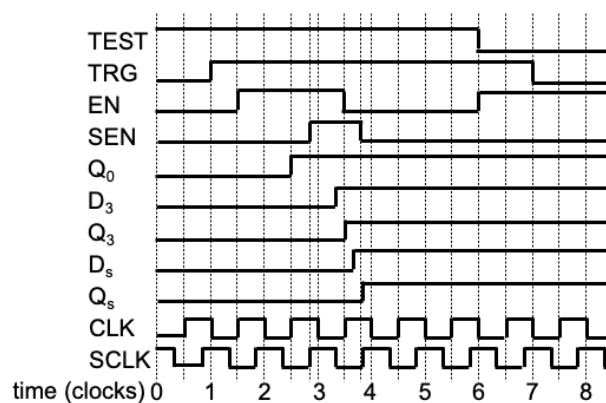


Fig. 2. Timing chart of a path delay test for proposed delay measurement.

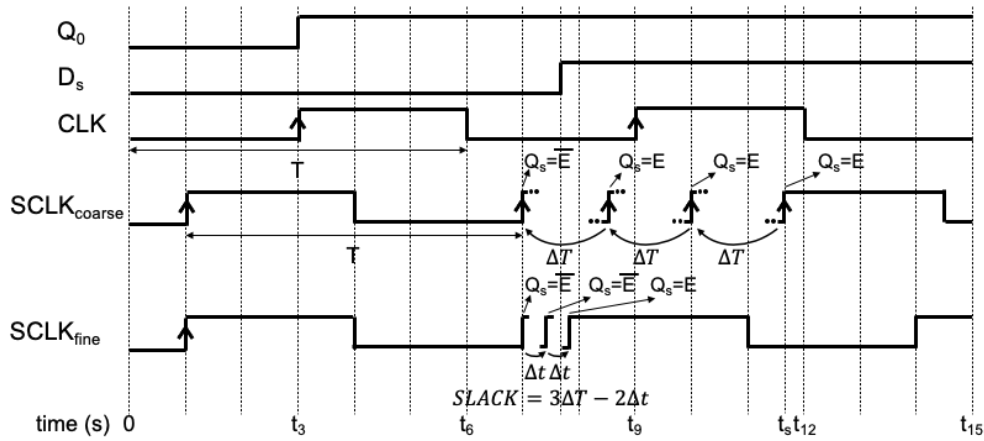


Fig. 3. Timing chart of proposed delay measurement with consecutive path delay test.

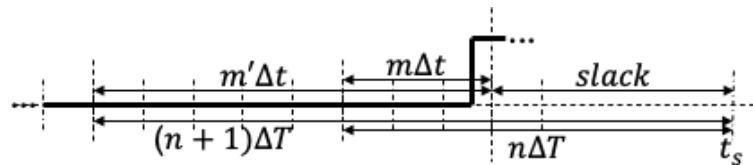


Fig. 4. Relation among m , m' , Δt , and ΔT .

2.2 MUX Chain for Fine Phase Shift

Figure 5 illustrates the 4-stage MUX chain used for the backward fine phase shift of the proposed slack measurement. We explain the MUX chain with this example. The clock input and the output are IN and OUT, respectively. The control input SEL controls the delay of the path between IN and OUT. The MUX chain is composed of an internal 4-stage 2-to-1 MUX chain and a redundant 2-to-1 MUX, which are serially connected. Each input of SEL is connected to the corresponding control input S_i of each i th stage. The symbol d_{i0} is the delay of the upper input wire of the i th stage and d_{i1} is that of the bottom wire of the internal MUX. The input of the internal MUX chain is IN_0 . The input IN_0 is also the output of the redundant MUX. The redundant MUX is controlled by the CAL input. The inverted OUT is feedback to an input of the redundant MUX. When $CAL = 0$, an external clock is launched from IN. When $CAL = 1$, a ring oscillator is constructed. The oscillation counter counts the oscillation times. The output is $COUNT_{OSC}$. The reference counter is used for calculation of the oscillation frequency of the ring oscillator whose output is $COUNT_{REF}$. The bold line is the path for the clock signal. The narrow line is redundant negative feedback path for the measurement of delay of the path for the clock signal. To make phase shift function, the fan-out routing of input wires of each 2-to-1 MUX of the internal MUX chain are routed as randomly as possible. For example, let d_{00} , d_{01} , d_{10} , d_{11} , d_{20} , d_{21} , d_{30} , d_{31} be 0.56 ns, 0.40 ns, 0.54 ns, 0.58 ns, 0.48 ns, 0.50 ns, 0.56 ns, 0.50 ns, respectively. The delay from IN to OUT depends on the control input SEL. For example, when $S_0S_1S_2S_3 = 0011, 0010, 0110$, the propagation delay values are 2.10 ns, 2.16 ns, 2.20 ns, respectively.

When the target resolution is 50 ps, the initial phase is 2.10 ns, and the range is 100 ps, the ideal phases are 2.10 ns, 2.15 ns, and 2.20 ns, respectively. Consequently, we can perform the phase sweep up from 2.10 ns to 2.20 ns with the 50 ps resolution in 10 ps maximum phase error. This multiplexer can be used as a fine phase shifter whose resolution is about 50 ps and the range is 100 ps. As the number of the stage of the internal MUX chain increases, the resolution becomes higher and the range becomes wider because the number of paths of the MUX chain increases exponentially. In the modern VLSIs, the difference of delay specification between a real chip and the simulation is unavoidable. Therefore, we must measure the delay of the paths from IN to OUT.

We measure it constructing the ring oscillator including the path. When $CAL = 1$, a ring oscillator composed of the path from IN to OUT (bold line) and a redundant path (narrow line) is constructed. By measuring the oscillation frequency, we can get the approximated delay of the path.

We count the time that the ring oscillator oscillates with the reference counter. When the time is $COUNT_{REF}$ and the oscillation times of the ring oscillator is $COUNT_{OSC}$, the oscillation period of the ring oscillator T_{OSC} (s) is $(COUNT_{REF}/COUNT_{OSC}) \cdot f_{REF}^{-1}$, where f_{REF} (Hz) is the clock frequency of the reference counter. Let $t_{sim}(SEL)$ (s) be the simulated delay of the path from IN to OUT when the control input is SEL. Let t_{fb_sim} (s) be the simulated delay of the redundant feedback path including inverter and redundant MUX delay. When the difference of the delay from IN to IN_0 from the delay from another input of the redundant MUX to IN_0 is negligible, $t_{MUXC}(SEL)$ (s), which is the delay from IN to OUT when the control input of the MUX chain is SEL, can be expressed as following formula.

$$t_{MUXC}(SEL) = \frac{t_{sim}(SEL)}{t_{sim}(SEL)+t_{fb_sim}} \cdot T_{OSC} = \frac{1}{1+t_{fb_sim}/t_{sim}(SEL)} \cdot \frac{COUNT_{REF}}{COUNT_{OSC}(SEL)} \cdot f_{REF}^{-1} \quad (2)$$

where $COUNT_{OSC}(SEL)$ is the value of $COUNT_{OSC}$ after calibration when the control input of the MUX chain is SEL. The values $t_{sim}(SEL)$ and t_{fb_sim} are obtained from the post layout simulation. Fabricated chips have both die-to-die variation and within-die variation. However, because the area of MUX chain is small, within-die variation does not affect the ratio $t_{fb_sim}/t_{sim}(SEL)$ of (2) very much. Die-to-die variation also does not affect the ratio very much because $t_{fb_sim}/t_{sim}(SEL)$ is the ratio of two paths inside a small circuit. Consequently, the calculated value $t_{MUXC}(SEL)$ is robust to process variations.

To sweep up the phase with the MUX chain, the appropriate control input sequence should be applied. Here the number of the stages of the MUX chain is assumed to be N. Let SEL'_K ($0 \leq K < M$) be the Kth control input in phase sweep up with resolution Δt . In this case, SEL'_K ($0 < K < M$) is a SEL that $|t_{MUXC}(SEL) - (t_{MUXC}(SEL'_0) + K\delta t)|$ is minimum in the set of SEL, where SEL'_0 is an arbitrary SEL that gives the initial phase and the variable δt (s) is the target time step of the delay of the MUX chain for the phase shift up.

Fig. 6 shows the ideal backward fine phase shift with every δt when the M control inputs $SEL'_0, \dots, SEL'_{M-1}$ are consecutively applied to the N-stage MUX chain.

Ideally, δt is equal to the fine resolution Δt . However, an oscillation counter is connected to the ring oscillator for the calibration. It works as a load during the oscillation. Consequently, the oscillation period is slightly different from that without the oscillation counter. Accordingly, $t_{MUXC}(SEL)$ calculated with (2) is slightly slower than the true value. It yields the slight difference between δt and Δt .

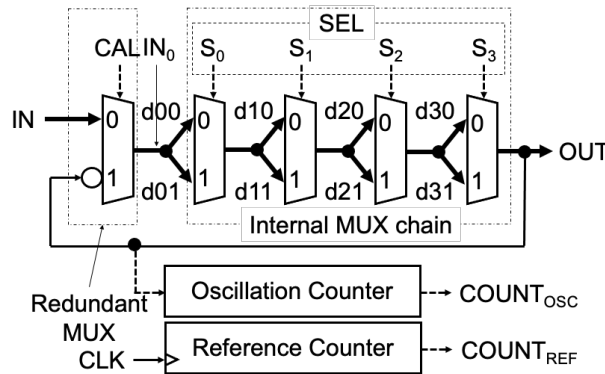


Fig. 5. 4-stage MUX chain for fine phase shift.

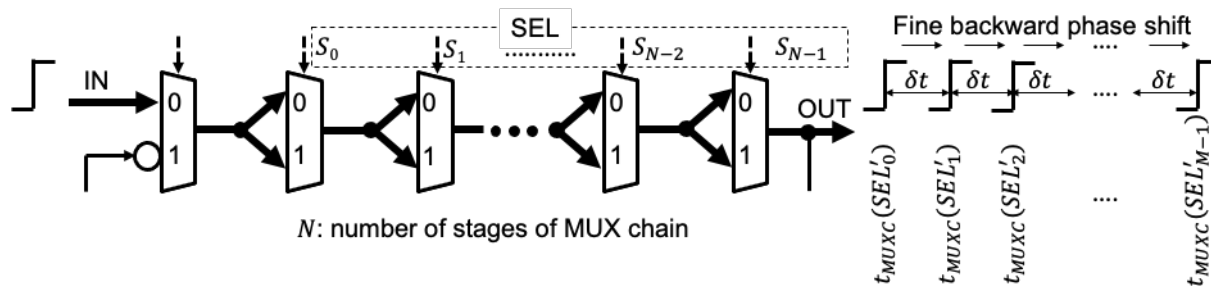


Fig. 6. The ideal backward fine phase shift with every δt with consecutive application of the M control inputs $SEL'_0, \dots, SEL'_{M-1}$ to the N -stage MUX chain.

2.3 Scheme of Proposed Online Delay Measurement

The proposed online slack measurement scheme is as follows.

- Step 1. Execute path delay test with the initial capture timing of SDFP and get the expected value E and initialize m and n to zero.
- Step 2. Shift phase forward by $2\pi\Delta T/T$ and increment n .
- Step 3. Execute path delay test.
- Step 4. If test response is equal to \bar{E} , go to Step 5, otherwise go to Step 2.
- Step 5. Shift phase backward by $2\pi\Delta t/T$ and increment m .
- Step 6. Execute path delay test.
- Step 7. If the test response is equal to \bar{E} go to Step 5, otherwise the slack is $n\Delta T - m\Delta t$.

3. Experimental Results

On AMD Artix-7 on Digilent Basys 3, we implemented the proposed method to the full-scanned s9234, which is an ISCAS89 benchmark circuit [12]. We measured the slack of the single-path sensitizable path which has the maximum unit delay. A shadow Flip-Flop was added to observe the end point of the path. The LOC test pattern for the path delay test was generated with an in-house Automatic Test Pattern Generator (ATPG). The test pattern was applied from a softcore MicroBlaze to the circuit through the single scan chain [13]. We used Vivado v2023.1 and Vitis v2023.1 for the implementation [14,15]. The external oscillator MicroChip DSC1033 sent 100 MHz clock signal to the circuit [16]. The RMS jitter of the clock signal was 12.8 ps at 100 MHz [16]. Figure 7 depicts the experimental environment. Figure 8 shows the zoomed Basys 3 Artix-7 FPGA board. The chip surrounded by the white edged square is the AMD Artix-7 XC7A35T-1CPG236C. For precise evaluation, the resolution of the coarse phase shift was rather higher. The coarse phase shift function was implemented with the cascaded 8 IDELAYs [17]. The reference clock frequency of the IDELAYs was 300 MHz to set the average tap delay 52 ps [18]. In this evaluation, the average tap delay was assumed to be the true tap delay. In this case, the range of variable delay of the IDELAY chain was 19.3 ns. Considering the typical phase resolution of the PLL on AMD FPGAs, the forward coarse phase shift resolution ΔT was set to 104 ps which is the delay of 2 taps. As the clock period of the clock signal was 10 ns, the region of the range of the IDELAY chain 9.3 ns – 19.3 ns was used. The number of the stage of the MUX chain for the fine phase shift was 16. The calibration time was 8,192 clocks. Table 1 shows the wire delay of the 16-stage MUX chain obtained from the post layout simulation. According to the simulation result, the minimum delay was 11.9 ns, the maximum delay was 14.2 ns, and the difference was 2.3 ns.

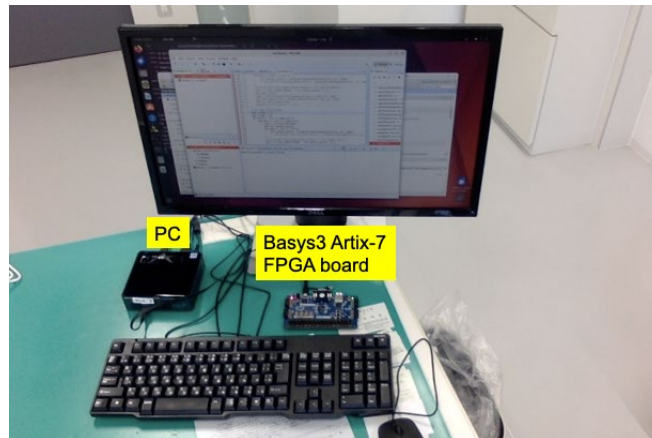


Fig. 7. Experimental environment: Basys 3 Artix-7 FPGA board and PC.

Table 1. Wire delay of each stage of 16-stage MUX chain d_{ij} (ps).

$j \backslash i$	0	1	2	3	4	5	6	7	8	9	10	11	12	13	14	15
0	953	975	779	892	596	975	779	892	707	975	778	892	596	975	778	892
1	827	869	948	605	707	774	948	718	826	774	843	718	707	869	843	718

i : stage number, j : selected path of MUX



Fig. 8. Experimental environment: Zoomed Basys 3 Artix-7 FPGA board.

3.1 Resolution

We evaluated the resolution of the backward fine phase shift. We calculated the set of SEL' for the backward fine phase shift when $\delta t = 50$ ps and 100 ps, respectively. Before the calculation, the smallest 100 samples, and the largest 100 samples were removed to keep the linearity. From the remaining SEL set, we obtained the sets of SEL' and calculated Δt s from (1). The clock signal contained 12.8 ps RMS jitter. To remove the jitter, we measured Δt 2,048 times consecutively and calculated the average value of them. We regard it as the pseudo-true Δt . Table 2 shows the result. When $\delta t = 50$ ps, $\Delta t = 10.1$ ps. It is 9.7 % of ΔT which is equal to the resolution of the conventional method in this evaluation. According to [4,5], this resolution is enough for detection and analysis of aging phenomena. The last column shows the phase step of the method from [8]. It is the one of the PLL of Altera Cyclone III FPGA (EP3C16F484C6N). It is almost equal to the coarse phase step ΔT of the proposed method or more than it.

3.2 Linearity

We evaluated the linearity of the backward fine phase shift. In general, the differential non-linearity at digital code k $DNL(k)$ when the resolution is τ is given by $DNL(k) = 1 - \frac{\Delta\tau_k}{\tau}$. In case of the proposed MUX chain, $\tau = \delta t$ and $\Delta\tau_k = t_{MUXC}(SEL'_k) - t_{MUXC}(SEL'_{k-1})$. Therefore, $DNL(k)$ is given by

$$DNL(k) = 1 - (t_{MUXC}(SEL'_k) - t_{MUXC}(SEL'_{k-1}))/\delta t \quad (3)$$

The integral non-linearity at digital code k $INL(k)$ is given by

$$INL(k) = \sum_{l=1}^k DNL(l) \quad (4)$$

Table 3 shows the evaluation result of the DNL and INL. When $\delta t = 50$ ps, the minimum/maximum DNL are -0.0047/0.0039 LSB, respectively. The minimum/maximum INL are 0.000014/0.0047 LSB, respectively. When $\delta t = 100$ ps, the minimum/maximum DNL are -0.0022/0.0023 LSB, respectively. The minimum/maximum INL are 0.000029/0.0023 LSB, respectively. Consequently, the absolute values of DNL and INL of the proposed fine phase shift is less than 0.005 LSB.

Table 2. Resolution of backward fine phase shift Δt (ps).

δt (ps)	Δt (ps)	ΔT (ps)	$\Delta t/\Delta T$ (%)	Δt (ps) [8]
50	10.1	104	9.7	96-208
100	24.2	104	23.3	

Table 3. DNL and INL of backward fine phase shift (LSB).

δt	Δt	DNL (LSB)		INL (LSB)	
		min	max	min	max
50	10.1	-0.0047	0.0039	0.000014	0.0047
100	24.2	-0.0022	0.0023	0.000029	0.0023

3.3 Precision of Measurement

We evaluated the precision of the backward fine phase shift. Averaging with multiple measurements reduces jitters in the measurement system. Here, we evaluated the effect of the averaging on the precision of the measurement. We measured the slack of the path 2,048 times. We regarded the average of them as the pseudo-true slack. We measured the slack and the averaged slack with 2, 4, 8, 16, and 32-time measurements 32 times respectively, and calculated the σ s in all the cases. The fine resolution Δt was set to 10.1 ps. Figure 9 plots them. The horizontal axis is the number of measurements to get the averaged σ . The vertical axis is the averaged σ (ps). The σ decreases as the number of the measurement increases. To let 3σ be less than Δt , more than 4 times measurements for averaging are required.

4. Conclusions

This paper has presented a fine delay measurement using forward and backward phase shift for online failure prediction and analysis. In the proposed method, a simple logic circuit for fine delay measurement is added to the conventional path delay measurement with phase-shift PLL to realize fine delay measurement. We confirmed that the proposed method realizes fine resolution in the order of 10 ps. It is about 10 % of the resolution of the conventional methods. The absolute values of DNL and

INL are less than 0.005 LSB. They are enough to detect and analyze aging phenomena which occurs inside the logic circuits of modern VLSIs.

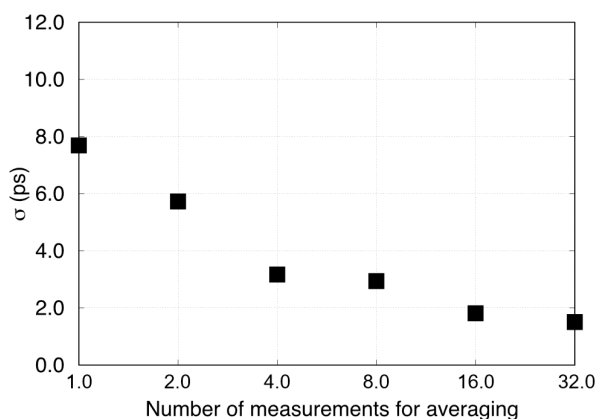


Fig. 9. Effect of averaging on σ of measurement result.

References

- [1] L. Anghel and F. Cacho, “Design-time exploration for process, environment and aging compensation techniques for low power reliable-aware design”, *IEEE Trans. on Emerging Topics in Comput.*, Vol. 10, No. 2, pp. 581-590, Apr.-Jun. 2022.
- [2] L. Anghel, A. Benhassain, A. Sivadasan, F. Cacho and V. Huard, “Early system failure prediction by using aging in situ monitors: Methodology of implementation and application results”, *Proceedings of VTS2016* (Las Vegas, NV, USA) May 2016.
- [3] Y. Miyake, T. Kato, S. Kajihara, M. Aso, H. Futami, S. Matsunaga and Y. Miura, “On-chip delay measurement for degradation detection and its evaluation under accelerated life test”, *Proceedings of IOLTS2020* (Napoli, Italy) Jul. 2020.
- [4] M. Sadi, L. Winemberg and M. Tehranipoor, “A robust digital sensor IP and sensor insertion flow for in-situ path timing slack monitoring in SoCs”, *Proceedings of VTS2015* (Napa, CA, USA) Jun. 2015.
- [5] A. Benhassain, F. Cacho, V. Huard, S. Mhira, L. Anghel, C. Parthasarathy, A. Jain and A. Sivadasan, “Robustness of timing in-situ monitors for AVS management”, *Proceedings of IRPS2016* (Pasadena, CA, USA) Apr. 2016.
- [6] K. Katoh, K. Namba, and H. Ito, “An on-chip delay measurement technique using signature registers for small-delay defect detection”, *IEEE Trans. on Very Large Scale Integr. Syst.*, Vol. 20, No.5, pp. 804-817, Jan. 2012.
- [7] Y. Sato, S. Kajihara, T. Yoneda, K. Hatayama, M. Inoue, Y. Miura, S. Ohtake, T. Hasegawa, M. Sato and K. Shimamura, “DART: Dependable VLSI test architecture and its implementation”, *Proceedings of ITC2012* (Anaheim, CA, USA) Nov. 2012.
- [8] J.M. Levine, E.A. Stott, G.A. Constantinides and P.Y.K. Cheung, “Online measurement of timing in circuits: for health monitoring and dynamic voltage & frequency scaling”, *Proceedings of FCCM2012* (Toronto, ON, Canada) Jul. 2012.
- [9] K. Katoh and K. Namba, “Time-to-digital converter-based maximum delay sensor for on-line timing error detection in logic block of very large scale integration circuits”, *Sensors and Materials*, Vol. 27, No. 10, pp. 933-943, 2015.

- [10] *Vivado Design Suite 7 Series FPGA and Zynq 7000 SoC Libraries Guide*, AMD Inc. (CA, USA), <https://docs.xilinx.com/r/en-US/ug953-vivado-7series-libraries/Introduction>
- [11] *Delay Fault Testing for VLSI Circuits*, A. Krstic and K.-T. Chen, Kluwer (Norwell, MA, USA), https://docs.xilinx.com/v/u/en-US/ug471_7Series_SelectIO
- [12] *Digilent Reference Programmable Logic Basys3*, Digilent Inc. (WA, USA), <https://digilent.com/reference/programmable-logic/basys-3/start>
- [13] *AMD MicroBlaze Processor*, AMD Inc. (CA, USA), <https://www.xilinx.com/products/design-tools/microblaze.html>
- [14] *Vivado Design Suite*, AMD Inc. (CA, USA), <https://www.xilinx.com/products/design-tools/vivado.html>
- [15] *Vitis Unified Software Platform*, AMD Inc. (CA, USA), <https://www.xilinx.com/products/design-tools/vitis.html>
- [16] *DSC1033 Data Sheet*, MicroChip Inc. (Arizona, USA).
- [17] *7 Series FPGAs SelectIO Resources User Guide*, AMD Inc. (CA, USA), https://docs.xilinx.com/v/u/en-US/ug471_7Series_SelectIO
- [18] *Artix-7 FPGA Data Sheet*, AMD Inc. (CA, USA), https://docs.xilinx.com/v/u/en-US/ds181_Artix_7_Data_Sheet